Acta Mech 212, 271–281 (2010)
DOI 10.1007/s00707-009-0258-0

Jianke Du · Kai Xian · Yook-Kong Yong · Ji Wang

SH-SAW propagation in layered functionally graded piezoelectric material structures loaded with viscous liquid

Received: 11 May 2009 / Revised: 26 October 2009 / Published online: 20 December 2009

Abstract We investigate the properties of shear horizontal surface acoustic wave propagation in layered functionally graded piezoelectric material structures loaded with viscous liquid. The piezoelectric material is polarized in the z-direction and the material properties change gradually along the thickness of the layer. Interfacial mechanical conditions are continuity of particle velocity and stress components at the interface. We here assume that the liquid is electrically insulated and its permittivity is much less than that of the piezoelectric material. The solutions of dispersion relations are obtained for insulated liquid with electrically open or shorted conditions by means of transfer matrix method. The effects of the gradient variation of material constants on the phase velocity and attenuation are presented and discussed in detail. The analytical method and the results are useful for the design of the resonators and sensors.

1 Introduction

Since White invented the interdigital transducers (IDTs) utilized for transmitting and receiving surface acoustic wave (SAW) signals in 1965, SAW has been applied successfully to the electronic industry with filters, delay lines, resonators, and oscillators for signal processing [1]. As we know, a new-style material called functionally graded material (FGM) was proposed to solve problems in the thermal-protection systems of aerospace structures in 1980s. Since then, FGM has attracted interest of investigators from many engineering disciplines. Today, functionally graded piezoelectric materials (FGPMs) can be manufactured and used in SAW devices to improve the efficiency and other features. Hence, the research of wave propagation behaviors and characteristics in FGPM has become a topic of practical importance. Qian et al. [2,3] investigated the transverse SAW in FGPM materials. Liang and Shen [4] studied the SH-SAW in layered piezoelectric structure by means of the transfer matrix method. Han and Liu [5] analyzed the characteristics of waves and transient responses in FGM cylinders by means of a hybrid numerical method (HNM). Liu and Wang [6] and Liu et al. [7] investigated Love waves in functionally graded piezoelectric structure using WKB method. Li et al. [8] studied the behaviors of Love waves in a layered functionally graded piezoelectric structure using the WKB method with different model. Du et al. [9] investigated analytically Love wave propagation in FGPM layers in which the distribution of material properties are assumed to be the same exponential function.

J. Du (✉) · K. Xian · J. Wang
Department of Mechanics and Engineering Science, School of Engineering,
Ningbo University, 818 Fenghua Road, Ningbo, Zhejiang 315211, China
E-mail: dujianke@nbu.edu.cn; jiankedu@gmail.com
Tel.: +86-574-87600074
Fax: +86-574-87608358

J. Du · Y.-K. Yong
Department of Civil and Environmental Engineering, Rutgers University,
623 Bowser Road, Piscataway, NJ 08854, USA

SAW devices may be immersed in a viscous liquid in many sensor applications. Attenuation of the SAW modes and leakage of energy into the liquid have to be considered in designing appropriate devices. The development of micro-acoustic wave sensors in biosensing or chemical sensing created the need for further investigations of the surface wave propagation in a layered medium loaded with viscous liquid. A number of acoustic wave modes have been utilized for various sensor applications. The influence of a viscous liquid on acoustic waves propagating in elastic or piezoelectric materials has been studied by many researchers, which is of particular interest for development of liquid sensors. Zaitsev et al. [10] investigated the acoustic waves in piezoelectric plates bordered with viscous and conductive liquid. Guo and Sun [11] studied propagation of Bleustein–Gulyaev wave in 6 mm piezoelectric materials loaded with viscous liquid. Zhang et al. [12] studied the Bleustein–Gulyaev wave for liquid sensing applications.

Through extensive studies, it is well known that Love wave or SH-SAW liquid or gas sensors are remarkable microacoustic devices with high sensitivity, due to the acoustic energy concentration within a few wavelengths near the surface. Such devices are particularly useful for the measurement of density, viscosity, and acoustic-electric properties of liquids, or electric potential, magnetic potential of applied fields. The layered structures, for example, a thin film on a substrate, are currently adopted to achieve high performance for these devices. Numerous investigations have been undertaken for the characteristic analysis of Love waves in layered piezoelectric structures by researchers in various disciplines because of its important applications [13,14], but so far the investigation of SH-SAW in FGPM structures loaded with viscous liquid has not been reported.

In this paper, we investigate the characteristics of SH-SAW propagation in FGPM structures loaded with viscous liquid. The effect of gradient factor on the phase velocity and attenuation can be obtained by means of the transfer matrix method.

2 Problem formulation

The layered FGPM structure loaded with viscous liquid is illustrated in Fig. 1, where a half-space elastic substrate is covered by a thin FGPM layer loaded with viscous liquid. The piezoelectric material is polarized in the z-direction. In order to use the transfer matrix method, we divide the FGPM layer into n sublayers along the z-direction, and make sure that the thickness of each sublayer is far less than the wavelength of the SAW for enough precision. The thickness of the ith sublayer is h_i. Each sublayer can be regarded as homogenous because of quite small thickness. Assuming the waves propagate in the y-direction, the displacement components and the electric potential are given as

$$u = v = 0, \quad w = w\,(x, y, t)\,, \quad \phi = \phi\,(x, y, t), \tag{1}$$

where u, v and w are the displacement components in the x, y and z-direction, respectively; ϕ is the electric potential. For each piezoelectric sublayer, the equilibrium equations of elasticity without body forces and the Gauss' law of electrostatics without free charge are given as follows:

$$T_{ji,j} = \rho \ddot{u}_i, \quad D_{i,i} = 0, \quad i, j = 1, 2, 3, \tag{2}$$

where T_{ij} and D_i are the stress and electric flux density (electric displacement), respectively; ρ is the mass density. The subscript comma denotes a partial derivative with respect to the coordinates, and a superimposed

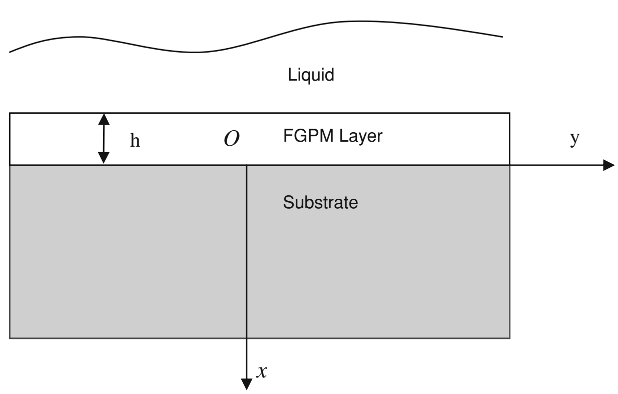

Fig. 1 A layered FGPM structure loaded with viscous liquid

dot represents the derivative with respect to time. For an anisotropic and linear electro-elastic solid, the coupled constitutive relation can be written as

$$
\begin{aligned}
T_i &= c_{ik} S_k - e_{ki} E_k, \\
D_i &= e_{ik} S_k + \varepsilon_{ik} E_k,
\end{aligned}
\tag{3}
$$

where S_k and E_k are the strain and electric field, respectively; c_{ij}, e_{ij} and ε_{ij} are the elastic, piezoelectric, and dielectric permittivity coefficients, respectively. It is obvious that various uncoupled equations can be deduced from Eq. (3) by setting the appropriate coefficients to zero. The extended strain–displacement relations are

$$
\begin{aligned}
&S_x = u_{,x}, \quad S_y = v_{,y}, \quad S_z = w_{,z}, \\
&S_{yz} = v_{,z} + w_{,y}, \quad S_{zx} = u_{,z} + w_{,x}, \quad S_{xy} = v_{,x} + u_{,y},
\end{aligned}
\tag{4a}
$$

$$
E_x = -\phi_{,x}, \quad E_y = -\phi_{,y}, \quad E_z = -\phi_{,z}. \tag{4b}
$$

For a linear and transversely isotropic electric-elastic medium with the poling direction along the z-axis, the material constant matrices of Eq. (3) can be written as

$$
[C] = \begin{bmatrix} c_{11} & c_{12} & c_{13} & 0 & 0 & 0 \\ & c_{22} & c_{23} & 0 & 0 & 0 \\ & & c_{33} & 0 & 0 & 0 \\ Sym. & & & c_{44} & 0 & 0 \\ & & & & c_{55} & 0 \\ & & & & & c_{66} \end{bmatrix}, \quad [e] = \begin{bmatrix} 0 & 0 & e_{31} \\ 0 & 0 & e_{32} \\ 0 & 0 & e_{33} \\ 0 & e_{24} & 0 \\ e_{15} & 0 & 0 \\ 0 & 0 & 0 \end{bmatrix}, \quad [\varepsilon] = \begin{bmatrix} \varepsilon_{11} & 0 & 0 \\ 0 & \varepsilon_{22} & 0 \\ 0 & 0 & \varepsilon_{33} \end{bmatrix}. \tag{5}
$$

Substituting Eqs. (4a) and (4b) into (3), then into (2) and making use of (5), the coupled wave equations and the constitutive equations can be reduced to

$$
c_{44}\nabla^2 w + e_{15}\nabla^2 \phi = \rho \tfrac{\partial^2 w}{\partial t^2}, \quad e_{15}\nabla^2 w = \varepsilon_{11}\nabla^2 \phi, \tag{6}
$$

$$
\begin{aligned}
T_{xz} &= c_{44} w_{,x} + e_{15}\phi_{,x}, \quad T_{zy} = c_{44} w_{,y} + e_{15}\phi_{,y}, \\
D_x &= e_{15} w_{,x} - \varepsilon_{11}\phi_{,x}, \quad D_y = e_{15} w_{,y} - \varepsilon_{11}\phi_{,y},
\end{aligned}
\tag{7}
$$

where $\nabla^2 = \frac{\partial^2}{\partial x^2} + \frac{\partial^2}{\partial y^2}$ is the two-dimensional Laplace operator in the Cartesian coordinates. By assuming

$$
\psi = \phi - \frac{e_{15}}{\varepsilon_{11}} w, \tag{8}
$$

Eq. (6) can be reduced further as

$$
c_{44}^* \nabla^2 w = \rho \frac{\partial^2 w}{\partial t^2}, \quad \nabla^2 \psi = 0, \tag{9}
$$

where c_{44}^* is given by

$$
c_{44}^* = c_{44} + \frac{e_{15}^2}{\varepsilon_{11}}. \tag{10}
$$

The displacement and electric potential in the substrate tend to zero far from the layer in the positive x-direction

$$
x \to +\infty, \quad w^{\mathrm{m}} = 0, \quad \phi^{\mathrm{m}} = 0, \tag{11}
$$

where the superscript m indicates the quantities in the substrate. Here, we think the liquid is nonconductive, so there are two typical cases being considered, namely, the electrically open and the shorted surface conditions. The electrically open case are written as

$$
\begin{aligned}
\dot{w}(-h, y, t) &= v^{\mathrm{L}}(-h, y, t), \\
\tau_{xz}(-h, y, t) &= \tau_{xz}^{\mathrm{L}}(-h, y, t), \\
D_x(-h, y, t) &= 0.
\end{aligned}
\tag{12}
$$

The electrically shorted case is given by

$$\begin{aligned} \dot{w}\left(-h, y, t\right) &= v^{\mathrm{L}}\left(-h, y, t\right), \\ \tau_{xz}\left(-h, y, t\right) &= \tau_{xz}^{\mathrm{L}}\left(-h, y, t\right), \\ \phi\left(-h, y, t\right) &= 0, \end{aligned} \tag{13}$$

where the superscript L indicates the quantities in the liquid. The continuous conditions at the interface between the piezoelectric layer and the elastic substrate are expressed as

$$\begin{aligned} w\left(0, y, t\right) &= w^{\mathrm{m}}\left(0, y, t\right), \quad T_{xz}\left(0, y, t\right) = T_{xz}^{\mathrm{m}}\left(0, y, t\right), \\ \phi\left(0, y, t\right) &= \phi^{\mathrm{m}}\left(0, y, t\right), \quad D_{x}\left(0, y, t\right) = D_{x}^{\mathrm{m}}\left(0, y, t\right). \end{aligned} \tag{14}$$

3 Solution of the problem

3.1 Solutions in the FGPM layer

The graded variations of material constants are diverse in practice and always designed to improve the properties of devices, such as graded elastic modulus, piezoelectric coefficient, and mass density, which we can analyze using the transfer matrix method. For simplicity and due to a limited length, we here assume and discuss two cases with the graded elastic modulus or graded piezoelectric coefficient varying as following functions:

$$c_{44} = c_{44}^{0}(1-\beta x)^{2}, \tag{15a}$$

$$e_{15} = e_{15}^{0}(1-\beta x)^{2}, \tag{15b}$$

where β is the graded factor. In the mean time, we assume that other material constants such as piezoelectric coefficient e_{15}, dielectric permittivity ε_{11}, and mass density ρ are homogenous along the thickness if we focus on the effect of graded elastic modulus, whereas we assume elastic modulus and other material constants are homogenous if we discuss the graded piezoelectric coefficient. The distribution functions such as Eqs. (15a) and (15b) indicate that the properties of materials near the surface of the structures are stiffer due to larger elastic modulus and piezoelectric coefficient. As we know this is impossible in practice, but it is helpful to investigate and understand the effect of the graded factor on the characteristics of the SH-SAW propagation. The solutions in the jth sublayer are expressed as

$$\left.\begin{aligned} w^{j} &= w^{j}\left(x\right)\exp\left[\mathrm{i}\xi\left(y-ct\right)\right] \\ \phi^{j} &= \phi^{j}\left(x\right)\exp\left[\mathrm{i}\xi\left(y-ct\right)\right] \end{aligned}\right. \quad \left(x\in\left[-(j-1)h/n, -jh/n\right]\right), \tag{16}$$

where ξ is the wave number and $\xi = \frac{\omega}{c}\left(1+\gamma\mathrm{i}\right) = k\left(1+\gamma\mathrm{i}\right)$. c and k are the phase velocity and the real part of the wave number in the y-direction, respectively. γ is the nondimensional attenuation coefficient, and ω is the angular frequency. Substituting Eq. (16) into (9), we can obtain

$$\begin{aligned} w^{j''}(x) + \xi^{2}(b_{1}^{j})^{2}w^{j}(x) &= 0, \\ \psi^{j''}(x) - \xi^{2}\psi^{j}(x) &= 0, \end{aligned} \tag{17}$$

where $(b_{1}^{j})^{2} = \frac{\rho c^{2}}{c_{44}^{*}} - 1$, c_{44}^{*} is given by

$$c_{44}^{*} = c_{44}^{j} + \frac{\left(e_{15}^{j}\right)^{2}}{\varepsilon_{11}}, \tag{18}$$

and superscript j indicates the quantities in the jth sublayer. From Eq. (15) we can obtain

$$c_{44}^{j} = c_{44}^{0}(1-\beta x)^{2}, \quad e_{15}^{j} = e_{15}^{0}, \quad \left(x=-jh/n\right), \tag{19a}$$

with graded elastic modulus, and

$$c_{44}^j = c_{44}^0, \quad e_{15}^j = e_{15}^0(1-\beta x)^2, \quad (x = -jh/n)\,, \tag{19b}$$

with graded piezoelectric coefficient. The solutions of Eqs. (17) are given by

$$\begin{aligned} w^j\,(x) &= C_1^j \cos(\xi b_1^j x) + C_2^j \sin(\xi b_1^j x), \\ \psi^j\,(x) &= C_3^j \mathrm{e}^{\xi x} + C_4^j \mathrm{e}^{-\xi x}, \end{aligned} \tag{20}$$

where C_1^j, C_2^j, C_3^j and C_4^j are unknowns to be determined. Then the displacement and electric potential in the jth sublayer can be expressed as

$$\begin{aligned} w^j\,(x,y,t) &= \left[C_1^j \cos(\xi b_1^j x) + C_2^j \sin(\xi b_1^j x)\right] \exp\left[\mathrm{i}\xi\,(y-ct)\right], \\ \phi^j\,(x,y,t) &= \left[C_3^j \mathrm{e}^{\xi x} + C_4^j \mathrm{e}^{-\xi x} + \frac{e_{15}}{\varepsilon_{11}}\left(C_1^j \cos(\xi b_1^j x) + C_2^j \sin(\xi b_1^j x)\right)\right] \exp\left[\mathrm{i}\xi\,(y-ct)\right], \end{aligned} \tag{21}$$

where $x \in \left(\frac{-(j-1)h}{n}, \frac{-jh}{n}\right)$.

We can obtain the continuous conditions across the interface of sublayers from (14) for $x_j = -hj/n$

$$\begin{aligned} w^j\left(x_j, y\right) &= w^{j+1}\left(x_j, y\right), \quad \tau_{xz}^j\left(x_j, y\right) = \tau_{xz}^{j+1}\left(x_j, y\right), \\ \phi^j\left(x_j, y\right) &= \phi^{j+1}\left(x_j, y\right), \quad D_x^j\left(x_j, y\right) = D_x^{j+1}\left(x_j, y\right). \end{aligned} \tag{22}$$

3.2 Solutions in the substrate and vacuum

The solutions of the displacement and the electric potential of waves in the substrate are given by

$$\begin{aligned} w^{\mathrm{m}} &= f^{\mathrm{m}}\,(x) \exp\left[\mathrm{i}\xi\,(y-ct)\right] = B_1^{\mathrm{m}} \mathrm{e}^{-\xi b^{\mathrm{m}} x} \exp\left[\mathrm{i}\xi\,(y-ct)\right], \\ \phi^{\mathrm{m}} &= B_2^{\mathrm{m}} \mathrm{e}^{-\xi x} \exp\left[\mathrm{i}\xi\,(y-ct)\right], \end{aligned} \tag{23}$$

where $b^{\mathrm{m}} = \sqrt{1 - c^2/\left(c_{\mathrm{sh}}^{\mathrm{m}}\right)^2}, \quad c_{\mathrm{sh}}^{\mathrm{m}} = \sqrt{c_{44}^{\mathrm{m}}/\rho^{\mathrm{m}}}$.

3.3 Solutions in the viscous liquid

The liquid is assumed to be viscous and nonconductive. Suppose the motion of the liquid is induced only by wave propagation in the piezoelectric material and also propagates in the form of harmonic wave. For this problem, the embroil inertial term in the Navier–Stokes equation can be omitted. Moreover, the pressure gradient also can be ignored since only shear deformation is considered during wave propagation. Therefore, the governing equation for the liquid is reduced as [15]

$$\mu^{\mathrm{L}} \nabla^2 v^{\mathrm{L}} = \rho^{\mathrm{L}} \dot{v}^{\mathrm{L}}, \quad \nabla^2 \phi^{\mathrm{L}} = 0, \tag{24}$$

where ρ^{L} is the mass density of liquid, μ^{L} is the dynamic viscous coefficient of the liquid and v^{L} is the liquid particle velocity in the z-direction. We consider the following solutions of Eq. (24):

$$\begin{aligned} v^{\mathrm{L}} &= v^{\mathrm{L}}\,(x) \exp\left[\mathrm{i}\xi\,(y-ct)\right], \\ \phi^{\mathrm{L}} &= \phi^{\mathrm{L}}\,(x) \exp\left[\mathrm{i}\xi\,(y-ct)\right]. \end{aligned} \tag{25}$$

Substitution of Eq. (25) into (24) and noticing the radiation conditions in the liquid far from the interface, we can obtain

$$v^{\mathrm{L}}\,(x) = D_1 \mathrm{e}^{\lambda x}, \quad \phi^{\mathrm{L}}\,(x) = D_2 \mathrm{e}^{\xi x}, \tag{26}$$

where $\lambda^2 = \xi^2 - \frac{\mathrm{i}\omega\rho^L}{\mu^L}$, $Re(\lambda) > 0$. D_1 and D_2 are unknown constants to be determined. The shear stress can be given by the Newtonian liquid law: $\tau_{xz}^{\mathrm{L}} = \mu^{\mathrm{L}} \frac{\partial v^{\mathrm{L}}}{\partial x}$.

4 The phase velocity equations

Defining the vector $\mathbf{C}^j = \left\{C_1^j, C_2^j, C_3^j, C_4^j\right\}^{\mathrm{T}}$, and substituting Eq. (21) into (22), we can obtain the relation of unknown constants to be determined between the jth and $(j+1)$th sublayer [16]

$$\mathbf{A}_j \mathbf{C}^j = \mathbf{B}_j \mathbf{C}^{j+1}. \tag{27}$$

Furthermore, this can be rewritten as

$$\mathbf{C}^{j+1} = \mathbf{B}_j^{-1} \mathbf{A}_j \mathbf{C}^j, \tag{28}$$

where $\mathbf{B}_j^{-1}$ is the inverse matrix of $\mathbf{B}_j$. Defining the matrix

$$\mathbf{D}_j = \mathbf{B}_j^{-1} \mathbf{A}_j, \tag{29}$$

it is obvious that $\mathbf{A}_j = \mathbf{B}_j$ for homogenous materials, and we can arrive at

$$\mathbf{C}^n = \overbrace{\mathbf{D}_{n-1}\mathbf{D}_{n-2}\cdots\mathbf{D}_2\mathbf{D}_1}^{n-1} \mathbf{C}^1. \tag{30}$$

From the conditions at the interface Eq. (14) we can obtain

$$\begin{aligned}
&C_1^1 - B_1^{\mathrm{m}} = 0,\\
&C_1^1 b_1^1 (c_{44}^1 + b e_{15}^1 - \mathrm{i}\eta_{44}\omega) + C_3^1 e_{15}^1 - C_4^1 e_{15}^1 = 0,\\
&b C_1^1 + C_3^1 + C_4^1 - B_2^{\mathrm{m}} = 0,\\
&C_2^1 b_1 (e_{15}^1 - b\varepsilon_{11}) - C_3^1 \varepsilon_{11} + C_4^1 \varepsilon_{11} - B_2^{\mathrm{m}} \varepsilon_{11}^{\mathrm{m}} = 0.
\end{aligned} \tag{31}$$

4.1 Solution of the electrically open conditions at the interface

From the stress and the electrically open conditions at the interface between liquid and piezoelectric layer (12), we can obtain the following:

$$\begin{aligned}
&\mathrm{i}\omega \cos(b_1^n h\xi) C_1^n + \mathrm{i}\omega \sin(b_1^n h\xi) C_2^n + D_1 \exp(-h\lambda) = 0,\\
&C_1^n b_1^n \xi \left(c_{44}^n + \left(e_{15}^n\right)^2 \big/ \varepsilon_{11}\right) \sin(b_1^n \xi h) + C_2^n b_1^n \xi \left(c_{44}^n + \left(e_{15}^n\right)^2 \big/ \varepsilon_{11}\right) \cos(b_1^n \xi h)\\
&\quad + C_3^n e_{15}^n \xi \exp(-\xi h) - C_4^n e_{15}^n \xi \exp(\xi h) - D_1 \mu^{\mathrm{L}} \lambda \exp(-h\lambda) = 0,\\
&\quad - C_3^n \exp(-h\xi) + C_4^n \exp(h\xi) = 0.
\end{aligned} \tag{32}$$

Noticing Eq. (30), we can regard Eqs. (31) and (32) as linear algebraic equations about the constants C_1^1, C_2^1, C_3^1, C_4^1, D_1, B_1^{m}, B_2^{m}. In order to obtain the nontrivial solutions of the above-mentioned unknown constants, the determinant of the coefficient matrix of these linear algebraic equations must equal zero. So the dispersive relations for the electrically open case can be obtained.

Table 1 Material coefficients of the piezoelectric $BaTiO_3$

c_{44}^0 (10^9 N/m^2)	e_{15}^0 (C/m^2)	ε_{11} (10^{-9} C^2/Nm^2)	ρ (10^3 kg/m^3)
43	11.6	11.2	5.8

Table 2 Material coefficients of SiO_2

c_{44}^{m} (10^9 N/m^2)	$\varepsilon_{11}^{\mathrm{m}}$ (10^{-9} C^2/Nm^2)	ρ^{m} (10^3 kg/m^3)
31.2	3.36	2.2

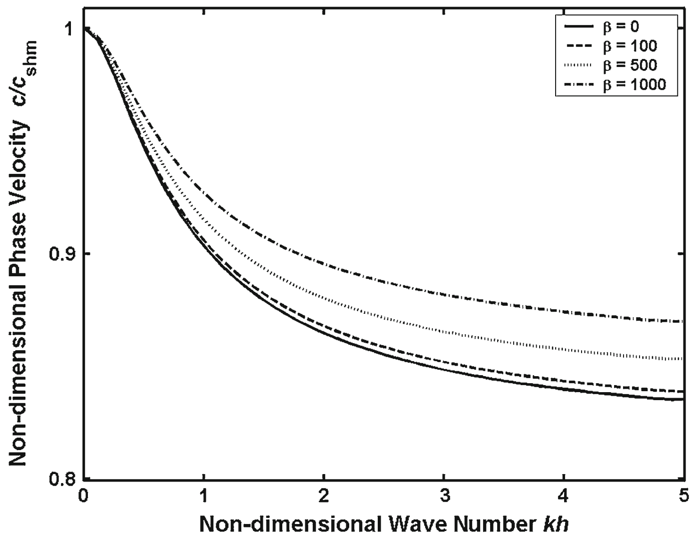

Fig. 2 Velocity of the first mode for electrically open case with graded elastic modulus

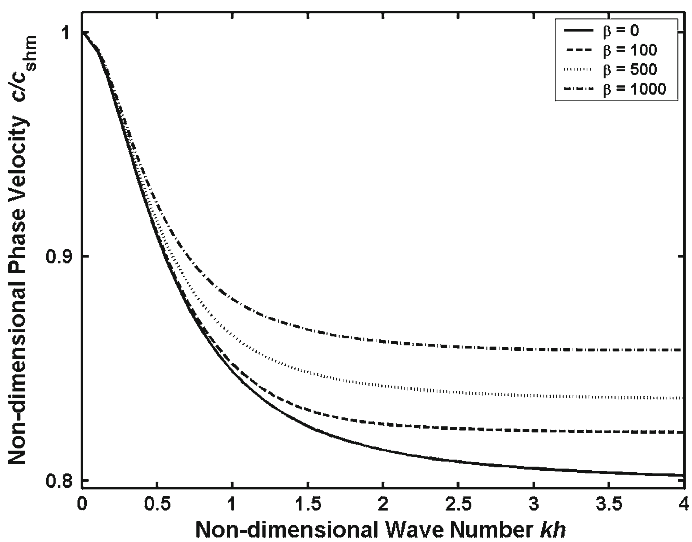

Fig. 3 Velocity of the first mode for electrically shorted case with graded piezoelectric coefficient

4.2 Solution of the electrically shorted conditions at the interface

From the stress and the electrically shorted conditions at the interface between liquid and piezoelectric layer (13), we can obtain the following:

$$\begin{aligned}
&\mathrm{i}\omega\cos(b_1^n h\xi)C_1^n + \mathrm{i}\omega\sin(b_1^n h\xi)C_2^n + D_1\exp(-h\lambda) = 0,\\
&C_1^n b_1\xi\left(c_{44}^n + \left(e_{15}^n\right)^2\big/\varepsilon_{11}\right)\sin(b_1^n\xi h) + C_2^n b_1^n\xi\left(c_{44}^n + \left(e_{15}^n\right)^2\big/\varepsilon_{11}\right)\cos(b_1^n\xi h)\\
&\quad + C_3^n e_{15}^n\xi\exp(-\xi h) - C_4^n e_{15}^n\xi\exp(\xi h) - D_1\mu^{\mathrm{L}}\lambda\exp(-h\lambda) = 0,\\
&C_1^n\frac{e_{15}^n}{\varepsilon_{11}}\cos(b_1^n h\xi) - C_2^n\frac{e_{15}^n}{\varepsilon_{11}}\sin(b_1^n h\xi) + C_3^n\exp(-h\xi) + C_4^n\exp(h\xi) = 0.
\end{aligned} \tag{33}$$

Similarly, Eqs. (31) and (33) can be rewritten as linear algebraic equations about C_1^1, C_2^1, C_3^1, C_4^1, D_1, B_1^{m}, B_2^{m}. So the dispersive relations for the electrically shorted case can be obtained by letting the determinant of the coefficient matrix of these linear algebraic equations equal zero.

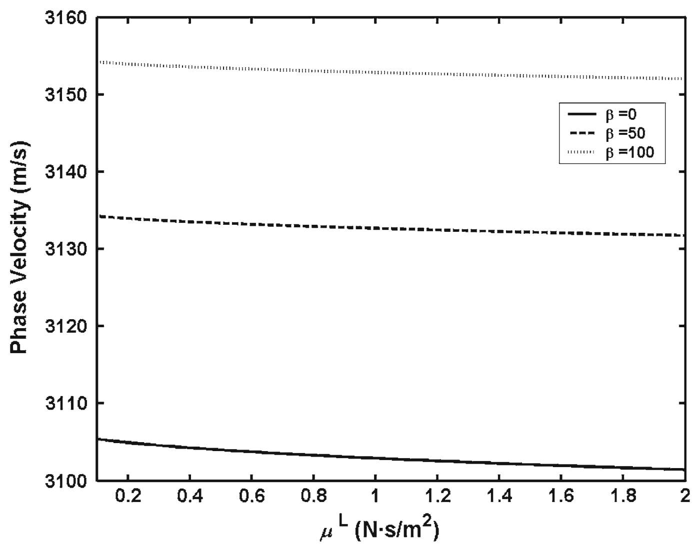

Fig. 4 Velocity of the first mode versus viscosity for electrically shorted case with graded modulus

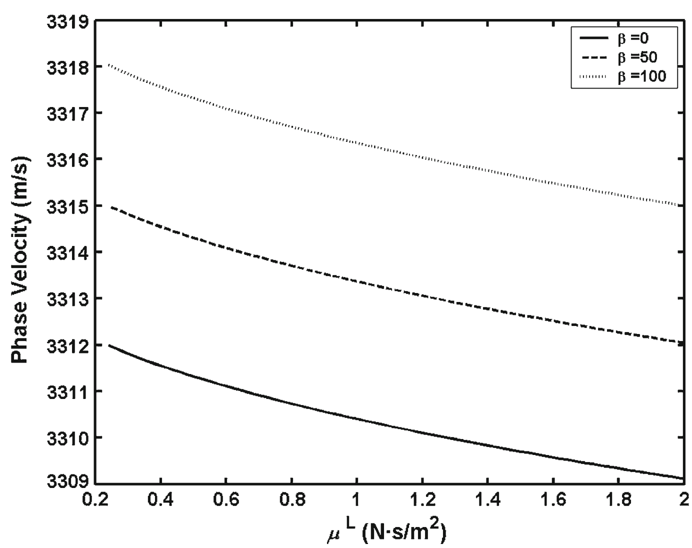

Fig. 5 Velocity of the first mode versus viscosity for electrically open case with graded piezoelectricity

5 Results and discussion

The material constants of FGPM layer and substrate are given in Tables 1 and 2. The thickness of the FGPM layer is $h = 0.1\,\text{mm}$. The FGPM layer is divided into more than 100 sublayers for the sake of enough precision while using transfer matrix method.

Figures 2 and 3 show the phase velocity of the first mode for the electrically open case with graded elastic modulus and shorted cases with graded piezoelectric coefficient, respectively, for $\mu^{\mathrm{L}} = 0.5\,\mathrm{N\,s/m^2}$. We can find the phase velocity increases with the graded factor, and decreases with increase of the nondimensional wavenumber.

Because the phase velocity is dispersive, we should discuss the effect of viscosity of liquid on phase velocity for the certain of wavenumber. Figures 4 and 5 present the phase velocity versus viscous coefficient for the electrically shorted case with graded elastic modulus and open case with graded piezoelectric coefficient, respectively, for $k = 15{,}000$. We can find the phase velocity decreases with increasing liquid viscosity. Furthermore, it can be seen that the curves for different β are almost parallel to each other, which means that graded variation of material properties cannot substantially improve the sensitivity of viscosity for this layered structure and graded distribution of materials.

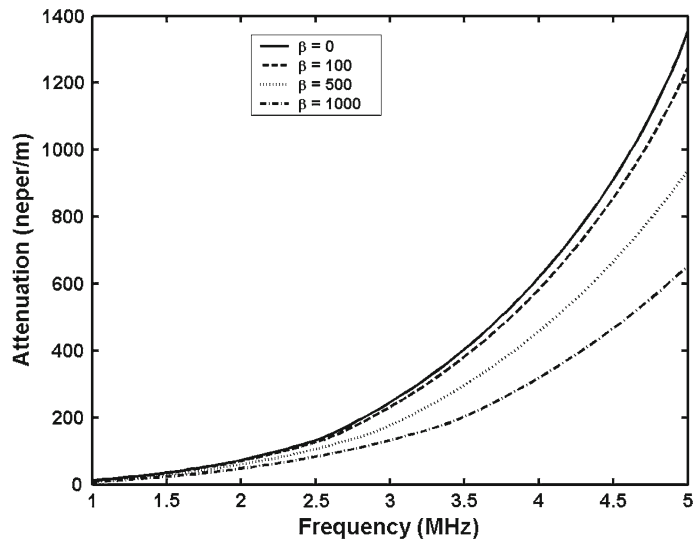

Fig. 6 Attenuation versus frequency for electrically open case with graded elastic modulus

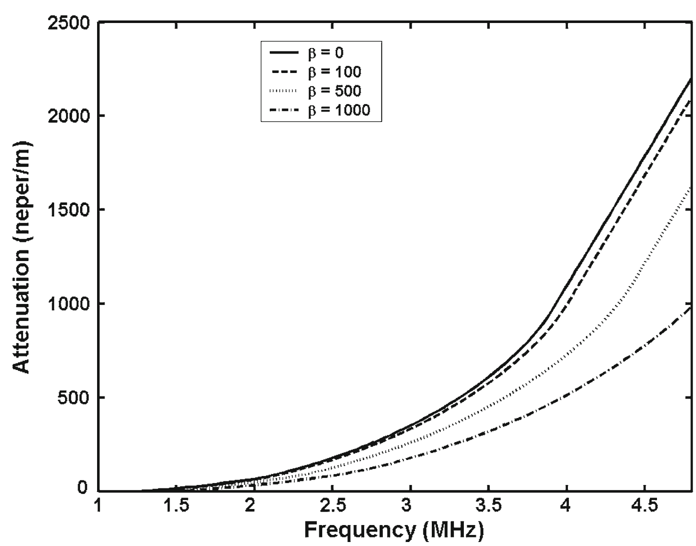

Fig. 7 Attenuation versus frequency for electrically shorted case with graded elastic modulus

Figures 6, 7, 8 and 9 show the attenuation versus frequency for graded elastic modulus and piezoelectricity with $\mu^{\mathrm{L}} = 0.5\,\mathrm{N\,s/m^2}$. It can be seen that the attenuation increases with the frequency. We also find that the graded factor of elastic modulus or piezoelectric coefficient has a remarkable effect on the attenuation for different frequency. It also can be seen that the attenuation decreases with the increase of the graded factor, and the relation is nonlinear between attenuation and the frequency. It is obvious that the attenuation is larger for a higher frequency. We can also change the graded distribution of material constants so as to obtain less attenuation for practical devices on the base of this point.

6 Conclusions

SH-SAW propagation in layered FGPM structures loaded with viscous liquid is studied in this paper. The solutions of dispersion relations are obtained for nonconductive liquid with electrically open and shorted conditions by means of the transfer matrix method. The effects of the gradient variation of elastic modulus and piezoelectric coefficient on the phase velocity and attenuation are presented and discussed in detail. From the results we can find that the phase velocity decreases with increase of the viscous coefficient. Furthermore, it can

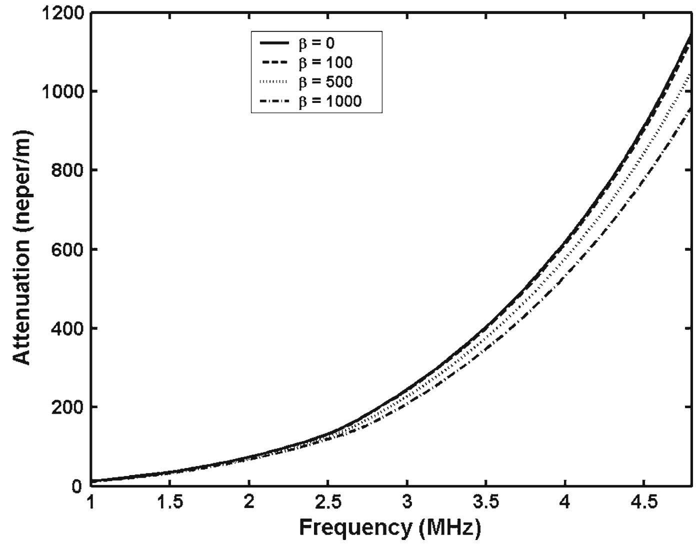

Fig. 8 Attenuation versus frequency for electrically open case with graded piezoelectric modulus

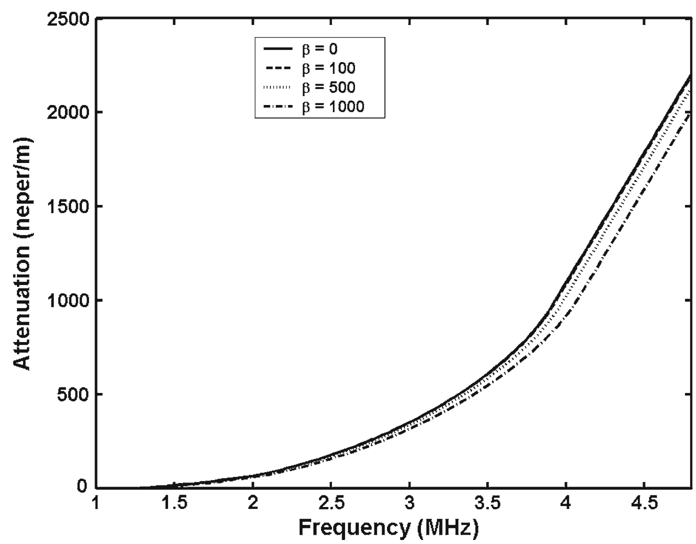

Fig. 9 Attenuation versus frequency for electrically shorted case with graded piezoelectric modulus

be seen that the attenuation increases with the frequency, the graded factor of elastic modulus or piezoelectric coefficient has a remarkable effect on the attenuation for different frequency, and the attenuation decreases with the increase of the graded factor. The analytical method and the results can be useful for the design of the resonators and sensors.

Acknowledgment The authors gratefully acknowledge the supports of the National Natural Science Foundation of China (Nos. 10772087 and 10932004), K.C. Wong Education Foundation, Hong Kong and K.C. Wong Magna Fund in Ningbo University.

References

1. White, R.M., Voltmer, F.M.: Direct piezoelectric coupling to surface elastic waves. Appl. Phys. Lett. **7**, 314–315 (1965)
2. Qian, Z.H., Jin, F., Wang, Z., Kishimoto, K.: Transverse surface waves on a piezoelectric material carrying a functionally graded layer of finite thickness. Int. J. Eng. Sci. **45**, 455–466 (2007)
3. Qian, Z.H., Jin, F., Lu, T.K., Kishimoto, K.: Transverse surface waves in functionally graded piezoelectric materials with exponential variation. Smart Mater. Struct. **17**, 065005 (2008)

4. Liang, W., Shen, Y.P.: Gradient surface ply model of SH wave-propagation in SAW sensor. Acta Mech. Sinica **15**(2), 155–163 (1999)
5. Han, X., Liu, G.R.: Elastic waves propagating in a functionally graded piezoelectric cylinder. Smart Mater. Struct. **12**(6), 962–971 (2003)
6. Liu, J., Wang, Z.K.: The propagation behavior of Love waves in a functionally graded layered piezoelectric structure. Smart Mater. Struct. **14**, 137–146 (2005)
7. Liu, J., Gao, X.S., Wang, Z.K.: Propagation of Love waves in a smart functionally graded piezoelectric composite structure. Smart Mater. Struct. **16**, 13–24 (2007)
8. Li, X.Y., Wang, Z.K., Huang, S.H.: Love waves in functionally graded piezoelectric materials. Int. J. Solids Struct. **41**, 7309–7328 (2004)
9. Du, J.K., Jin, X.Y., Wang, J., Xian, K.: Love wave propagation in functionally graded piezoelectric material layer. Ultra-Sonics **46**, 13–22 (2007)
10. Zaitsev, B.D., Kuznetsova, I.E., Joshi, S.G., Borodina, I.A.: Acoustic waves in piezoelectric plates bordered with viscous and conductive liquid. Ultrasonics **39**(1), 45–50 (2001)
11. Guo, F.L., Sun, R.: Propagation of Bleustein–Gulyaev wave in 6 mm piezoelectric materials loaded with viscous liquid. Int. J. Solids Struct. **45**(13), 3699–3710 (2008)
12. Zhang, C., Caron, J.J., Vetelino, J.F.: The Bleustein–Gulyaev wave for liquid sensing applications. Sens. Actuators, B: Chem. **76**(1–3), 64–68 (2001)
13. McMullan, C., Mehta, H., Gizeli, E., Lowe, C.R.: Modeling of the mass sensitivity of the Love wave device in the presence of a viscous liquid. J. Phys. D: Appl. Phys. **33**, 3053–3059 (2000)
14. Ke, L.L., Wang, Y.S., Zhang, Z.M.: Love waves in an inhomogeneous fluid saturated porous layered half-space with linearly varying properties. Soil Dyn. Earthq. Eng. **26**(6–7), 574–581 (2006)
15. Lee, Y.C., Kuo, S.H.: Leaky Lamb wave of a piezoelectric plate subjected to conductive fluid loading: theoretical analysis and numerical calculation. J. Appl. Phys. **100**(7), 073519-1-10 (2006)
16. Stewart, J.T., Yong, Y.-K.: Exact analysis of the propagation of acoustic waves in multilayered anisotropic piezoelectric plates. IEEE Trans. Ultrason. Ferroelectr. Freq. Control **41**(3), 375–390 (1994)